Evaluating a Radiation Monitor for Mixed-Field Environments based on SRAM Technology

Georgios Tsiligiannis, Luigi Dilillo, Alberto Bosio, Patrick Girard, Serge Pravossoudovitch, Aida Todri-Sanial, Arnaud Virazel, Julien Mekki, Markus Brugger, Frédéric Wrobel, et al.

15th INTERNATIONAL WORKSHOP ON RADIATION IMAGING DETECTORS
23–27 JUNE 2013,
PARIS, FRANCE

Evaluating a radiation monitor for mixed-field environments based on SRAM technology

G. Tsiligiannis,[a,1] **L. Dilillo,**[a] **A. Bosio,**[a] **P. Girard,**[a] **S. Pravossoudovitch,**[a] **A. Todri,**[a] **A. Virazel,**[a] **J. Mekki,**[b] **M. Brugger,**[b] **F. Wrobel**[c] **and F. Saigne**[c]

[a]*Laboratoire Informatique Robotique Electronique Montpellier (LIRMM),*
161 rue Ada 34095 Montpellier, France

[b]*CERN,*
1211 Geneve, Switzerland

[c]*Université de Montpellier II,*
Place Eugene Bataillon 34095 Montpellier, France

E-mail: tsiligiann@lirmm.fr

ABSTRACT: Instruments operating in particle accelerators and colliders are exposed to radiations that are composed of particles of different types and energies. Several of these instruments often embed devices that are not hardened against radiation effects. Thus, there is a strong need for monitoring the levels of radiation inside the mixed-field radiation areas, throughout different positions. Different metrics exist for measuring the radiation damage induced to electronic devices, such as the Total Ionizing Dose (TID), the Displacement Damage (DD) and of course the fluence of particles for estimating the error rates of the electronic devices among other applications. In this paper, we propose an SRAM based monitor, that is used to define the fluence of High Energy Hadrons (HEH) by detecting Single Event Upsets in the memory array. We evaluated the device by testing it inside the H4IRRAD area of CERN, a test area that reproduces the radiation conditions inside the Large Hadron Collider (LHC) tunnel and its shielded areas. By using stability estimation methods and presenting experimental data, we prove that this device is proper to be used for such a purpose.

---

[1]Corresponding author

Contents

1 Introduction

Throughout the particle accelerators and colliders different types of particles and energies are present along the different locations. In such environments, several instruments and other complex devices operate. Cost wise, they often embed electronic components that are not hardened against radiation effects. For this reason, but also for monitoring purposes, the levels of radiation along different positions of these facilities need to be well defined. There are several metrics to measure the levels of radiation such as the Total Ionizing Dose (TID), the Displacement Damage (DD) and finally the fluence of particles, with which the error rates of the devices can be extracted.

Several methods exist for measuring the different metrics that define the level of radiation damage induced to the devices. For instance, Gas Field Detectors [1] or solid state detectors [2] are used to calculate the fluence of ionizing particles. An example of a monitoring device used for estimating the levels of radiation in different positions in the LHC tunnel and its shielded areas is the RadMon [4]. This monitor uses a series of devices to estimate the different metrics (TID, DD, HEH fluence). RadMons are placed throughout the entire LHC tunnel and its shielded areas, providing quality information on the radiation levels (400 in different positions). A similar work is presented in [5], where the recorded SEUs are used to extrapolate the particle fluence by using SRAM memories of different technology nodes.

In this work, we take advantage of the sensitivity of memory devices to radiation to propose an SRAM based monitor that is able to provide a real-time estimation of the HEH fluence, based on the collection of Single Event Upsets (SEU) in memory devices. This monitor is capable of undergoing the CERN radiation zones without degradation, while providing accurate estimations of the HEH fluence based on the quantity of collected SEUs. This monitor has been evaluated for its functionality and its ability to provide accurate data under the H4IRRAD test area of CERN facilities and other CERN accelerators [6].

The rest of the paper is organized as follows: in section 2 a detailed analysis of the setup, the functionality and the data processing of the monitor is provided. Section 3 analyzes the methods that we used for retrieving accurate data and provide with reliable statistics. Finally, section 4 presents the retrieved data and the study on the different accuracy models that we developed and section 5 concludes the paper with a discussion on future work.

2 Monitor functionality

2.1 The monitor configuration

The monitor that we introduce is SRAM based and its functionality relies on the collection and interpretation of the occurring SEUs in the memory array. The specifications of the monitor were defined according to the radiation environment, the size of the memory, the technology node, the cross section of the memory, the power consumption, the speed and the latchup immunity of the component. The size and speed of the memory will define the easiness of SEU collection but also the read-back speed. Based on the size of the SRAM, the number of memory components has to be also defined, which will specify the size of the monitor. The power consumption is an important factor for the portability of the monitor, while the cross section shows the sensitivity of the device to radiative particles. We propose a monitor that integrates 3 low power commercial 32Mbit SRAMs of 90nm technology. As it will be shown later, the overall size of the memory array allows us to collect sufficient data in a small time span. Moreover, the 90nm technology node is a diffused technology for recent devices and we can also predict the error rates of these devices. Finally, the fact that this memory is commercial, makes it more sensitive towards radiation effects and consequently SEUs, working to the benefit of data collection.

As shown in in figure 1, the monitor is composed by three 32Mbit 90nm commercial SRAMs. The main functionality of the monitor is based on a Finite State Machine (FSM) which is responsible for the handling of the memories, but also for other functionalities of the monitor, such as communicating with the control computer. The FSM is implemented in a FLASH based FPGA, an intrinsic robust technology against radiation with respect to other SRAM based FPGAs. The memories share the same connections with the FPGA (address bus, data bus, read and write enable signals), besides the Chip Enable (CE) signals. This results to the access of only one memory for a read/write operation at a time. Additionally to the FPGA and the memories, an anti-latchup circuit is added to the board, protecting the electronic devices against possible latchup threats. Other circuits involve the clock generator, providing the FPGA with a clock signal at 50MHz and also a transceiver. The latter enables the communications and thus the calibration of the I/O signals between the FPGA and the computer according to the RS232 protocol. The transceiver is not visible in figure 1 since in order to reduce any possible sources of malfunction, the transceiver is located outside the beam room, in a safe area. Finally, a JTAG port, allows to program and reconfigure the FPGA, in order to study different setup modes for the monitor and perform measurements. Throughout this study, we consider particles above 20MeV, thus the plastic packaging of the memories embedded in the monitors will not affect the measurements since HEH will not be stopped by it.

There are two types of tests that are usually applied to memory components during radiation testing: static mode testing and dynamic mode testing. Static mode testing is extensively described
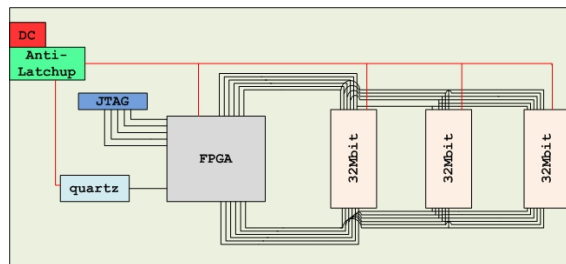
Figure 1. SRAM based monitor. Three 32Mbit SRAMs are integrated which are driven by a FLASH based FPGA. Additional circuitry is added to the board for latchup protection and the clocking of the FPGA. The transceiver circuitry is located outside the monitor board in a separate card.

Figure 2. (a) Multiple Cell Upset as a result of a particle induced current that spreads over several neighbouring cells. (b) Multiple Cell Upset as a result of a micro-SEL.

at the JEDEC standard [7] and it is the most common type of testing for memory components under particle beams. In static mode testing, the memory array is written with a known sequence (ex. all bits set to '1' or '0' or a checkerboard sequence), and after a certain time window the entire memory is read back. During the read-back, each read word is compared with the expected sequence and if any upset bit is detected, it is transmitted, along with the address of the word and the timestamp of the read-back time to the control computer. On the other hand, dynamic mode testing requires the continuous application of operations to the memory array during irradiation. Dynamic mode testing is usually applied to test the memory under more realistic conditions combined with static mode testing.

Static mode testing of the SRAMs is chosen instead of dynamic mode testing for this application for several reasons. These reasons lie on the fact that static mode testing provides data that are easier to process with respect to dynamic mode testing. While in static mode testing the memory remains in data retention mode and the only source of errors comes from the memory array, i.e. the cells themselves, in dynamic mode testing other sources of upsets may appear. Since in dynamic mode testing read/write accesses are acted in the memory, the peripheral circuits of the memory become sensitive to upsets. If a Single Event Transient (SET) is induced to the periphery of the memory, it may affect a large number of bit-cells of the memory array. This makes more difficult to identify the SEUs that induce Multiple Cell Upsets (MCUs). Although from many points of view such effects are interesting, for particle detecting applications these events are not desirable. In figure 2, two examples of MCU are displayed. Figure 2 (a) shows a typical MCU induced by a single particle involving 9 corrupted cells. This is the result of a parasitic current induced by a single impinging particle that is large enough to spread over several neighboring cells. MCUs share the same mechanism as the charge sharing between pixelated sensors as also mentioned in [8]. Figure 2 (b) shows an MCU event with a high number of corrupted cells (**530**). As reported in [9], figure 2 (b) event is the result of a micro Single Event Latchup (micro-SEL) in the partition of the
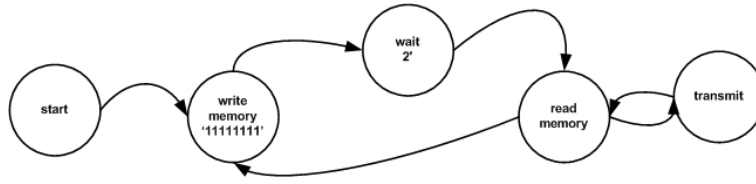
Figure 3. Finite State Machine responsible for the operation of the monitor. The memory is written with a known sequence, and after a defined time window the memory is read. The FSM transmits the upsets to a control computer.

array that is selected for the operation. Such kind of events have been observed when the memory was only in dynamic mode. However, even when the monitors operate static mode, besides the period in retention state the memories are read back for retrieving the occurring SEUs. Thus, it is possible to observe such phenomena exactly during the time windows needed for the read-back, when the memory is temporarily in dynamic mode. We will detail later how we take in account these MCUs as SEUs.

As already precised, the main functionality of this monitor is based on static mode testing, applied by an FSM. The schematic indicating the principal operations of this FSM is presented in figure 3. The data pattern that we chose to apply to the memory array is "all ones" sequence, while the retention time that we apply is a two minutes window between each read-back. However, since the FPGA of the monitor is reconfigurable, the data pattern and the time window between the read-backs of the memory can be modified, according to the needs of each experiment, as well as to calibrate the monitors.

2.2 Test area

The beam line in which we tested the proposed monitors is H4IRRAD, a test area of CERN facilities [6], in which electronic equipment operating at the CERN accelerators are tested. In H4IRRAD there are two different zones which incorporate different particle spectra: the internal zone in which a 400GeV/c proton beam is present; and the external zone, which is separated from the internal by a 20cm thick special concrete. The particle spectra given in [10] show that there is one order of magnitude difference between the HEH fluence of the internal zone and the external zone and thus, differences should be expected at the frequency of SEU occurrence in our monitors. The main contributors to SEUs are protons, pions and neutrons with energies above 20MeV. In addition, some SRAM memories and devices can be sensitive to thermal neutrons due to the presence of Boron [4]. Additional information on the particle spectra for the two different zones (i.e. internal/external) can be found in [6]. In the internal zone, pions and neutrons are the main contributors (49% and 40% respectively), while in the external zone neutrons are the main contributor (85%). We placed monitors in two different positions at the internal zone, and four monitors in two positions at the external zone (two monitors per position), providing us data for a total of six monitors. We calculated that a monitor in the internal zone received the maximum ionizing dose of 76Gy(or 7.6krad). The experiments lasted two weeks, receiving a total of a few 10^{10}HEH which is equivalent to a year of operation at the Large Hadron Collider tunnel and its shielded areas. The first days of the experiments, the intensity of the beam was increasing from a low level up to its highest value which

– 4 –
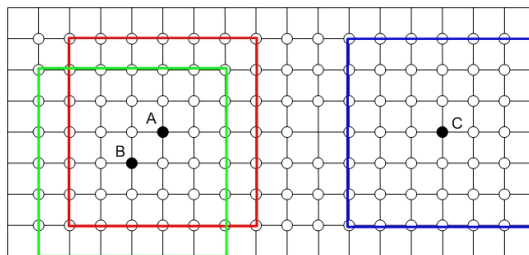
Figure 4. Clustering scheme of the applied algorithm to the data recorded during irradiation. Upsets 'A','B' and 'C' have the same timestamp. The squares indicate the maximum range of each cluster.

was maintained until the end of the experiments, allowing us to verify whether our monitors would sense this progressive increase to the HEH fluence. From measurements that we performed during and after the experiments, we found that the devices were not subjected to any kind of performance degradation as detailed later on.

2.3 Data processing

The data processing is based on an algorithm, which decodes the upsets placing them into clusters. The purpose of the algorithm is not just to count the SEUs, but also to extract the MCUs, and any other types of large scale disturbances, in order to obtain a consistent SEU count in the log file. When the memories were accessed for read and write operations, a scrambled addressing scheme was used by default by the manufacturer. The first step of the algorithm, is to decode the scrambled addresses and obtain the physical location of the affected cells. In the second step, the algorithm verifies whether two bit flips belong to the same time window that would indicate their possibility of belonging also to the same upset (the time window is predefined at two minutes).

The recorded SEUs are compared initially according to their timestamp, and following their location. In the case two upsets have a timestamp indicating that they were recorded at the same read-back of the memory, they are further verified with respect to their location. By treating extensive data from other campaigns, we consider as sufficient a three cell neighboring scheme. Figure 4 presents the clustering process, according to the physical location of the cells, considering that upset cells 'A','B' and 'C' shared the same timestamp. We can observe that the cluster of upset 'B' meets the cluster of upset 'A' and thus they will be merged to the same cluster and will be considered as one event. On the contrary, upset 'C' is too far, and thus we cannot include it to the same cluster of upsets 'A' and 'B'. Using this procedure, clusters with hundreds or even thousands of upset cells can be created as a result of MCUs or SELs. We have observed that this procedure is very sensitive and necessary since not taking into account the clustering can alter significantly the data. During one hour of recording, one monitor at the external zone detected *608* upsets, which correspond to a cross section of $8.9 \cdot 10^{-14} cm^2$. By applying the clustering tool (and thus suppressing MCUs, MBUs, micro-SELs etc), we found out that the actual detected events were *424* and this corresponded to a cross section of $6.2 \cdot 10^{-14} cm^2$.
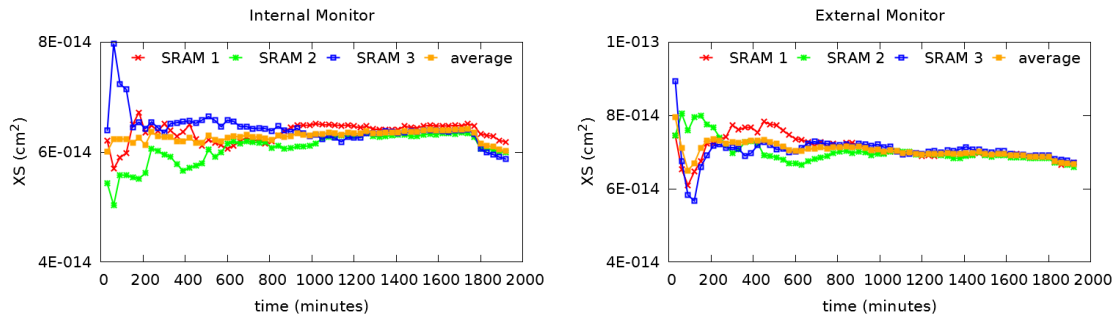
Figure 5. Cross section evolution as a function of time for two monitors at the internal and external zones. The cross section reaches a stable point after the accumulation of a few hundreds of upsets (200-300).

3 Characterization

Two of the main characteristics that a monitor entails are the reproducibility and the stability along the measurements. This means that under the same conditions the monitor must be able to provide the same results within an acceptable error margin. Depending on the intensity of radiation (i.e. the fluence of particles), the collection of SEUs plays an important role to the calculation of the bit cross section (XS). The bit cross section XS is defined as the number of errors divided by a given fluence of particles and the size of the memory ($XS = \#err/(\#particles + 32Mbit)$). The more the collected SEUs are, the more accurate the calculated XS is. In order to see at which point the number of collected SEUs is sufficient for the extraction of the HEH, the evolution of the cross section over time is given in figure 5.

Results in figure 5 show that after a relatively small time span (three hours) the XS converges to a stable value, approximately $7 \times 10^{-14} cm^2$. In some cases the graphs show that the XS value has fluctuations. This is normal if we take into account that the relative error of the HEH fluence calculated for each position is approximately $\pm 40\%$. When the number of accumulated SEUs that we used for the calculation of the cross section reached a concentration of 200-300 events, the cross section converges towards a stable value. Such numbers of collected SEUs can be achieved in approximately 30 minutes in the external zone and in less than 15 minutes in the internal zone, when the proton beam is fully operational.

When characterizing such a monitor an additional concern is the size of the memories. We have observed that a single memory device can converge very fast towards a stable cross section and thus, provide reliable results. In each monitor, we embedded three memories for two reasons. The first reason is to assist quantitatively the process of the handling of log disturbances, and the second is to accumulate a higher number of events in a smaller time window. From measurements that we applied, we discovered that employing more than three memories does not improve significantly the accuracy of the measurements at H4IRRAD. For lower HEH rates, we expect that a larger number of memories can be necessary, but it should be always estimated as a function of the cost, the power consumption and of course the space.
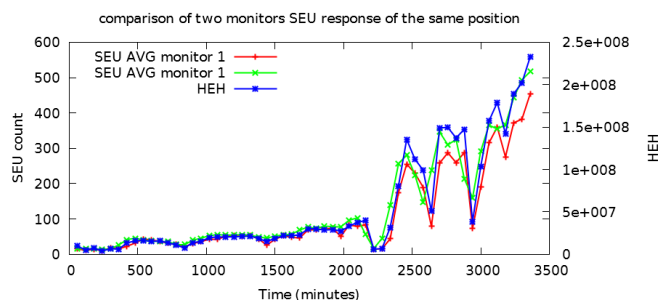
Figure 6. SEU response of two monitors placed at the same position. HEH fluence remains the same for both monitors since they belong to the same position.
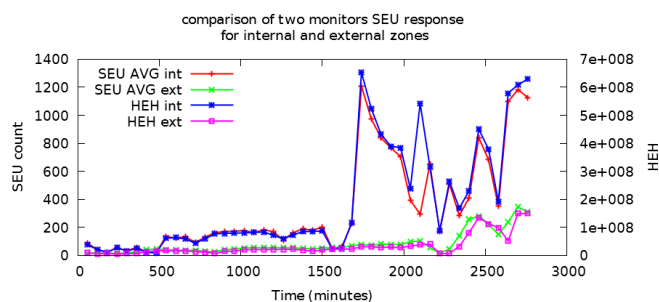
Figure 7. SEU response of two monitors in the internal and the external zones. The difference between the HEH fluence of the two zones is calculated to be approximately one order of magnitude.

4 Results

So far, we have shown that the proposed monitor is capable of providing reliable data based on the stability metrics that we presented. According to [10] the relation between the HEH and the SEUs is linear. The methodology presented in section 3 showed that the monitors are expected to be stable towards the recorded SEUs, with respect to the received HEH fluence. To prove this stability, we present in figure 6, the average of the recorded SEUs in the three SRAMs of each one of two monitors. Since the position is the same, it should be expected that the HEH fluence to be the same, and thus the recorded SEUs.

Figure 6 reveals that both monitors have a very good accordance with respect to the accumulated SEUs. Additionally, since the HEH and the SEUs are scaled equally in the graph, it can be seen that they follow the same increase, a result of the linearity behind these two metrics. Figure 7 expands this relation towards the internal and the external zones, and shows the differences in the recorded SEUs, with respect to the differences of the received HEH fluence at each position.

As it is depicted in figure 7, for both monitors at the internal and the external zones, the relation between the HEH and the recorded SEUs is linear and despite the differences in the particle spectra, between the two zones, the relation is not altered. Results show that a very good level of accordance between the recorded SEUs and the HEH fluence can be achieved in a relatively small time window (one hour). Figures 6 and 7 prove that the monitors can provide with a stable result even when the HEH fluence is relatively low ($\approx 10^6 HEH/hr$). Since the relation of the HEH and the recorded

SEUs is stable, these monitors could also be used to estimate whether a particle beam is properly calibrated and provides a stable flux.

5   Conclusions

We have presented an SRAM based monitor that was developed for the monitoring of the radiation levels and more particularly the HEH fluence of particle accelerators and other mixed radiation environments. These monitors can be potentially used in numerous applications, not only for the monitoring of the radiation levels, but also for particle beam calibrations. Several units of the monitor have been tested and characterized at the H4IRRAD test area of CERN facilities, and they have been proven to be suitable and reliable for facilities of similar types and energies of particles. Monitors can withstand a total ionizing dose of 76Gy, but further experiments should be performed for evaluating their operativeness with higher values of total ionizing dose. Additionally, further calibration of these monitors should be applied in the future with mono-energetic particle beams to better understand and estimate the contribution of alpha and low energy particles to the XS. Finally, this monitor could be tested and evaluated in the future in similar facilities around the world, such that to compare with already operating instruments of other radiation environments.

References

[1] G.F. Knoll, *Radiation detection and measurements*, John Wiley and Sons, Inc., New York 2000.

[2] P. Rehak, *Silicon radiation detectors*, *IEEE Trans. Nucl. Sci.* **51** (2004) 2492.

[3] R. Ballabriga et al., *Medipix3: A 64 k pixel detector readout chip working in single photon counting mode with improved spectrometric performance*, *Nucl. Instrum. Meth.* **A 633** (2011) S15.

[4] G. Spiezia et al., *The LHC Radiation Monitoring System - RadMon*, PoS(RD11)024.

[5] D. Makowski, M. Grecki, Andrzej Napieralski, S. Simrock and B. Mukherjee, *A distributed System for Radiation Monitoring at Linear Accelerators*, RADECS 2005, PI4-1.

[6] B. Biskup et al., *Commissioning and Operation of the H4IRRAD Mixed-Field Test Area*, CERN-ATS-Note-20110212 PERF.

[7] *Measurement and Reporting of Alpha Particle and Terrestrial Cosmic Ray-Induced Soft Errors in Semiconductor Devices*, *JEDEC Test Standard* No. 89, (2001).

[8] X.X.Cai and S.P. Platt, *Modeling Neutron Interactions and Charge Collection in the Imaging Single-Event Effects Monitor*, *IEEE Trans. Nucl. Sci.* **58** (2011) 910.

[9] J. Tausch, D. Sleeter, D. Radaelli and H. Puchner, *Neutron Induced Micro SEL Events in COTS SRAM Devices*, *Radiation Effects Data Workshop* (2007).

[10] G. Tsiligiannis et al., *SEU Monitoring in Mixed-Field Radiation Environments of Particle Accelerators*, RADECS 2013.

[11] K. Roed et al., *Method for measuring mixed field radiation levels relevant for SEEs at the LHC*, RADECS 2011.